Composites: Part A 190 (2025) 108667

Contents lists available at ScienceDirect

Composites Part A

journal homepage: www.elsevier.com/locate/compositesa

Recycling carbon fibers by solvolysis: Effects of porosity and process parameters

Daniele Tortorici [a], Yi Chen [b], Leon Mishnaevsky Jr [b], Susanna Laurenzi [a,*]

[a] Department of Astronautical Electrical and Energy Engineering, Sapienza University of Rome, Via Salaria 851-881, Rome 00138, Italy
[b] Department of Wind Energy, Technical University of Denmark, Roskilde, Denmark

HIGHLIGHTS

- Uncured regions enhance depolymerization with fewer cross-links.
- Voids increase surface area, accelerating solvolysis.
- Higher temperatures and higher fiber content boost solvent diffusivity.
- Lower solvent concentration reduces depolymerization efficiency.
- Model predicts solvolysis based on diffusion and dissolution dynamics.

ARTICLE INFO

Keywords:
Solvolysis
Carbon fiber composites
Composites recycling
Finite element simulation

ABSTRACT

Chemical recycling, also known as solvolysis, is one of the most promising strategies for recycling fiber-reinforced thermosetting composite materials, due to its ability to recover nearly undamaged fibers for reuse. This approach is particularly appealing for carbon fibers, which have a high environmental production cost. However, there is a lack of understanding of the modelling and optimization of reaction conditions that would be required for the widespread use of this technology. This study explores how different solvolysis conditions and manufacturing-induced porosity influence the efficiency of the solvolysis process in epoxy-based carbon fiber composites. The goal is to enhance understanding of the process to enable more efficient material recovery. A comprehensive series of experiments was conducted, varying solvolysis process parameters, fiber volume fractions in the composites, and solvent concentrations. The effects of voids within the composite materials on solvolysis efficiency were investigated through numerical analysis, incorporating an anisotropic diffusion coefficient into the model. The results reveal that the quality of the material significantly affects the overall rate of solvolysis. The findings suggest that understanding the role of voids and the relationship between composite quality and solvolysis can improve the efficiency of composite recycling, contributing to more sustainable life-cycle management of these materials.

1. Introduction

The management of end-of-life components made of composite materials has garnered significant and increasing interest. Composites, which are multiphase materials that combine and exploit the characteristics of their constituent materials, are specifically designed to achieve targeted performance outcomes for various applications. Although, the use of composites dates back to ancient time, their application has notably expanded in recent decades due to advancements in chemistry [1–3]. This expansion has benefitted numerous sectors, including automotive, industrial, wind energy, and aerospace industries [4–7]. The typical lifetime of composites ranges from several years to a few decades [8,9], leading to an increase in composite waste that mirrors historical production trends. For instance, it is estimated that thousands of aircraft will be retired in the near future [10], and wind power sector will generate approximately 40 million tons of blade waste by 2050

Abbreviations: HTP, High temperature and pressure; LTP, Low temperature and pressure; CFRP, Carbon fiber-reinforced polymer; rCF, Recycled carbon fibers; PC, Processing conditions; RMSE, Root mean square error.

* Corresponding author.
E-mail address: susanna.laurenzi@uniroma1.it (S. Laurenzi).

https://doi.org/10.1016/j.compositesa.2024.108667
Received 4 October 2024; Received in revised form 5 December 2024; Accepted 14 December 2024
Available online 16 December 2024

[11].

Composites are material developed to be resistant, durable and suited for application in demanding environments [1,2,12–14]. However, these advantages now present challenges in waste treatment through established recycling strategies [15]. Consequently, new technologies are being developed to treat composite wastes and reduce their environmental impact. These technologies can be categorized into three principal methods: mechanical recycling, heat-based treatment (pyrolysis), and chemical treatment (solvolysis) [15–21]. In mechanical recycling, waste is shredded, cut, and reduced to powder form to be incorporated as filler in new materials [22,23]. The other two methods seek to depolymerize the matrix of the composite material to separate its constituent phases: the matrix itself and the reinforcement, typically glass or carbon fibers. This separation enables the recycling and reuse of these components individually [18].

The literature extensively discussed both the advantages and disadvantages of the various recycling strategies. Mechanical recycling is characterized by lower costs but yields lower-value recycled products [19,23]. Pyrolysis can produce high-quality recycled fibers [24,25] and the liquid/gaseous by-products can also provide value [18,20]. Downsides, it requires high temperatures (from 400-450 °C or greater to mitigate the char formation) [17,20,24–26] and typically results in fibers that are short, discontinuous and fluffy. Solvolysis, on the other hand, can operate at lower temperatures [21] and produce longer fibers with good-retained properties [18,27–32]. Solvolysis can be categorized basing on the operative conditions in terms of temperature and pressure. Oliveux et al. [21] distinguish between high temperature and pressure (HTP) conditions when $T > 200$ °C and $P > 1$ atm, and low temperature and pressure (LTP) when $T < 200$ °C and $P = 1$ atm. In LTP applications an acid medium is predominantly used [28–30] while in HTP the solvents in critical or near critical conditions are chosen. In this case alcohols, acetone, water or combination of those are used [31–33]. This preference arises because, under critical conditions, chemicals with reduced environmental impact and safety concerns, such as water and alcohols, can act as solvents for polymers. On the other hand, reaching HTP conditions requires significant energy and expensive equipment [21,33]. For instance, the critical point of water is reached at 374 °C and about 22 MPa [34].

From a cost perspective, solvolysis can be expensive due to the need for specialized solvents, substantial energy input, and the handling of chemical waste. However, advances in solvent efficiency and recycling of solvents themselves could reduce these costs over time. In terms of feasibility, solvolysis has demonstrated promising results for various composite materials, but scaling the process to an industrial level remains a significant challenge [17,35]. Key hurdles include optimizing the reaction conditions for different composite formulations and ensuring that the recovered fibers and resins meet the quality standards necessary for reuse. Scalability is also limited by the availability and cost of solvents, as well as the energy-intensive nature of the process, especially when HTP conditions are used [33]. Nevertheless, with ongoing research and technological advancements, solvolysis could become a viable option for large-scale, sustainable recycling of composite materials in the future [35].

Taking stock of the various recycling processes, this study focuses on low-temperature processing LTP solvolysis, as it offers significant benefits in terms of recovered material and environmental impact, especially when the liquid part is recovered and carbon fiber-reinforced polymers (CFRPs) are treated to reclaim and reuse carbon fibers.

Recycled carbon fibers (rCF) by solvolysis can indeed have a reduced global warming potential and require less energy compared to the production of virgin fibers [17,27,36,37]. Additionally, other environmental impact indicators may also be improved, as highlighted by a study building on the authors' previous research [29]. Many studies have centered on using recycled carbon fibers in new composites. Oliveux et al. [38] reported the first attempt in literature of rCF reuse by solvolysis in composites, documenting very good properties in comparison to the virgin fibers-based composites. Hao et al. [39], used an acetic acid and zinc acetate aqueous buffer to recycle a CFRP waste and then used rCF to produce a new composite that retained 90 % of the tensile strength and 82 % of the tensile modulus when compared to a control sample made of virgin fibers. The successful adoption of rCF recycled by solvolysis is also observed in other contexts, including carbon/carbon composites [40], additive manufacturing [41] and space applications [42]. Other researchers have instead focused their efforts on studying solvolysis through numerical analysis, highlighting the critical role of computational modeling in assessing and enhancing this recycling method. Luo et al. [43] investigated how solvolysis parameters impact its efficiency, presenting findings from a combined experimental and numerical study. Chen et al. [44] focused on the various governing physical mechanisms, such as solvent diffusion within the polymer matrix, phase transition from solid polymer to solution, and the movement of the solid/liquid boundary. They pointed out that the quality of composites may influence the recycling process.

The objective of this study is to advance the understanding of solvolysis as a recycling method by investigating various aspects of the solvolysis process. First, we focused on how the quality of the material at the time of recycling influences the solvolysis process. Specifically, we examined the effects of both the degree of cure and porosity of the composites on solvolysis yield, defined as the weight percentage of depolymerized epoxy. To achieve this, we fabricated composites under different processing conditions (PC) to simulate end-of-life composites. Epoxy resin was chosen due to its widespread use in thermosetting composites. We varied the curing temperature and time from the datasheet values and estimated the degree of cure for each condition using an analytical model implemented in MATLAB, which was calibrated using known data about the epoxy. This model was also employed to estimate the size and number of voids, based on literature assumptions regarding typical initial void radius and void content percentage. Samples of neat epoxy cured under different processing conditions were subjected to LTP solvolysis for varying durations. The solvolysis yield was determined after drying the samples to characterize the time-dependent behavior of the process. Subsequently, we analyzed how various recycling treatment parameters, including temperature and solvolysis fluid concentration (sulfuric acid diluted with demineralized water), impacted the results. Additionally, the effect of fiber volume fraction (V_f) in the composites was investigated by producing and treating samples with two different V_f levels and comparing the results to those of neat cured epoxy samples. In parallel, a finite element model of solvolysis for pure resin samples was developed to correlate experimental findings with model parameters and create a predictive tool. The model utilized a three-layer scheme to simulate solvent diffusion into the polymer and its dissolution. The parameters identified were then applied to develop a second finite element model that accounted for the presence of voids and fibers, providing insights into how these factors affect solvolysis yield from a numerical perspective. This approach offers theoretical guidance and enables extensive analysis without the need for costly and time-consuming practical trials, thus accelerating the development and optimization process.

2. Experimental part

2.1. Materials and sample preparation

The epoxy resin PRIME 37 from Gurit (Wattwil, Switzerland) was selected for this study due to its low-toxicity and suitability for industrial applications such as the wind and marine ones. This two-part system offers a range of hardeners, allowing users to choose an appropriate working time and cure speed. For this study, the slow hardener was selected to provide sufficient pot life for samples production, with a mixing ratio of 100:29 parts by weight as specified in the datasheet.

Tenax-E IMS65 E23 unidirectional carbon fiber yarns from Teijin (Tokyo, Japan) with an epoxy-compatible sizing were used for the

Table 1
Details of the samples used during the experimental campaign, including processing conditions, composition, and quantity.

Processing conditions for samples manufacturing	Notation	Composition	Number of samples
7 h – 65 °C	PC 1	Neat epoxy	84 samples
7 h – 65 °C	PC 1	Composite 14 %V_f	20 samples
7 h – 65 °C	PC 1	Composite 28 %V_f	16 samples
7 h – 50 °C	PC 2	Neat epoxy	48 samples
72 h – 23 °C	PC 3	Neat epoxy	48 samples

reinforced samples.

Samples were produced under three different processing conditions. The curing process involved an ambient pressure cure in an oven, starting at room temperature (23 °C) with a temperature increase of 3 °C per min until reaching the target curing temperature. The specific conditions were as follows: PC 1 involved a 7-h cure at 65 °C, PC 2 a 7-h cure at 50 °C, and PC 3 a 72-h cure at 23° C. The samples were cured in a custom-built silicon mold, forming bars 150 mm in length, with a short edge of 13 mm and a thickness of 4 mm. After curing, the bars were cut into samples measuring 13 mm × 13 mm × 4 mm. A total of 216 samples were produced. Table 1 provides the specifications of the samples used in the experiments, outlining the processing conditions during curing, the composition, and the quantity of samples produced.

Epoxy samples were produced using all the three-cure schedule mentioned, while for the composites we used PC 1 condition. Composites were produced with fiber volume fractions of 14 % and 28 %. To achieve the desired amount of reinforcement, a precision balance (accurate to 10^{-4} g) was used, along with product density data from the datasheet and the final composite dimensions. Carbon fibers yarns were stacked in 7 and 14 layers to achieve the fiber volume percentage of 14 % and 28 % respectively.

Fig. 1 presents pictures and schemes of the samples. Specifically, Fig. 1a depicts an epoxy bar before cutting, including a SEM image of a superficial void. Fig. 1b displays a composite bar (V_f = 14 %) with the scheme of its cross-section, illustrating the lamination sequence. Voids are represented as red dots in the schematic. Porosity in composite materials refers to regions not filled with resin or fiber. Achieving zero porosity is extremely challenging due to various contributing factors. Common sources of voids include trapped air, volatiles, off-gassing, and leaks in tools or vacuum bags, all of which can elevate porosity levels [45]. To address this, a degassing phase was introduced prior to resin curing to minimize void content. An analytical balance (model CPA225D, Sartorius, Gottingen, Germany) with a precision of 0.01 mg and an accuracy of ± 0.03 mg was employed to measure the density of materials using the specific measurement kit (Density determination kit, model YDK01, Sartorius, Gottingen, Germany). The polymeric samples exhibited a measured density of 1.148 ± 0.002 g/cm^3, which is slightly lower than the datasheet value of 1.160 g/cm^3. This discrepancy indicates a porosity level of approximately 1 %.

2.2. Solvolysis process

Solvolysis was carried out using sulfuric acid aqueous solutions prepared by dilution with demineralized water. Three different concentrations were investigated: 18 mol L^{-1}, 17 mol L^{-1}, and 16 mol L^{-1}. These values were selected starting with the highest concentration available, then progressively analyzing lower concentrations to minimize acid usage. Previous studies have shown that a concentration of 15 mol L^{-1} dissolves the matrix very slowly [46]. Therefore, the focus was placed on intermediate concentrations of 16 and 17 mol L^{-1}, in addition to the highest concentration. An extensive experimental campaign was conducted to characterize the progression of solvolysis over time, using four to five-time intervals ranging from 1 h to the total time required to complete solvolysis (which varies depending on other parameters, as detailed later). The influence of the composite's manufacturing processing conditions (denoted as PC 1, 2, and 3) was investigated, as both the final degree of cure and void content — dependent on these conditions — can affect solvolysis yield. Furthermore, the effects of the solvolysis temperature (85 °C, 115 °C, and 145 °C) was studied. For a selected case (PC 1, 115 °C), the influence of solvolysis fluid

Table 2
Summary of experiments conducted to characterize solvolysis, detailing material composition, processing conditions, and solvolysis parameters.

Type of samples	Processing conditions for samples manufacturing	Solvolysis parameters		
		Concentration (mol/L)	Temperature (°C)	Times (h)
Epoxy	7 h – 65 °C	18	85, 115, 145	1 to 24
Epoxy	7 h – 50 °C	18	85, 115, 145	1 to 24
Epoxy	72 h – 23 °C	18	85, 115, 145	1 to 17
Composite 14 %V_f	7 h – 65 °C	18	115	1 to 16
Composite 28 %V_f	7 h – 65 °C	18	115	1 to 9
Epoxy	7 h – 65 °C	16, 17, 18	115	1 to 48

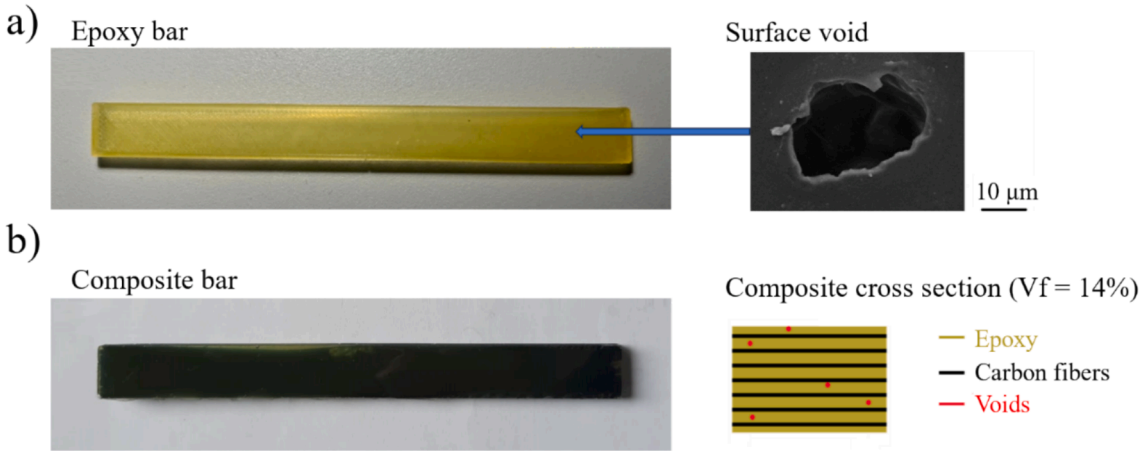

Fig. 1. Cured epoxy bar (a) and composite bar (b) before cutting. (a) the image shows a void captured via scanning electron microscopy at 5000 × magnification; (b) includes a schematic of the composite lamination sequence for V_f = 14 %, with voids represented as red dots.

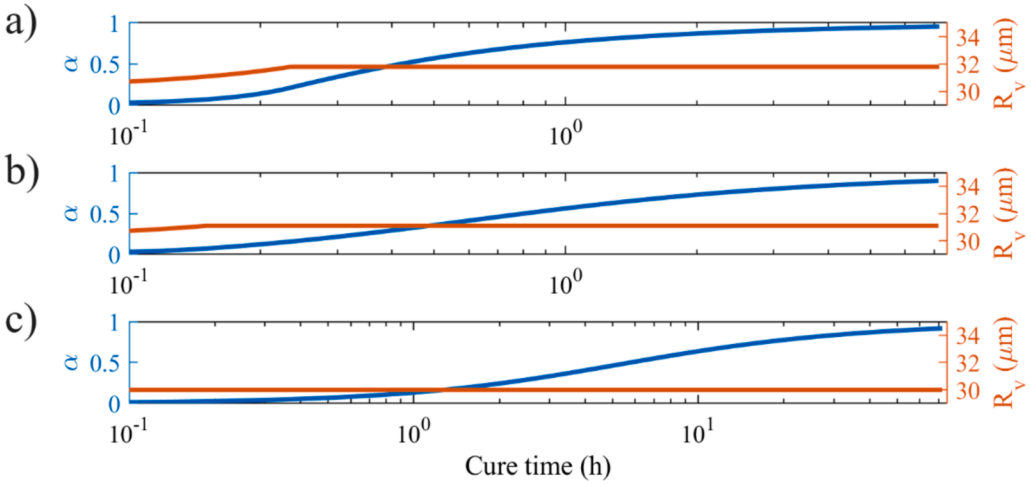

Fig. 2. Time profiles for degree of cure (blue) and void radius (red), during the curing process conditions: 7 h – 65 °C (a), 7 h – 50 °C (b), and 7 h – 23 °C (c).

concentration (18 mol L^{-1}, 17 mol L^{-1}, and 16 mol L^{-1}) and reinforcement volume fraction (0 %, 14 %, and 28 %) was also examined. Table 2 summarizes the parameters for each experimental set. Each experiment was replicated four times to ensure repeatability.

The experiments were conduct by immersing each sample in a beaker containing 20 ml of acid at varying concentrations and temperatures, the latter obtained using a heating plate and measured with an infrared thermometer. Samples were weighted with a precision balance (accurate to 10^{-4} g) prior to the treatment. After solvolysis, samples were dried in an oven at 50 °C for 24 h before being weighted again. The depolymerized mass percentage W was calculated by weight difference, referring to the pre-treatment value W_0.

Data are collected at various solvolysis times (t) and fitted with a two-component model. The first component represents the solvent uptake by the polymer, which occurs immediately as the samples are immersed in the solvolysis fluid. The second component corresponds to the dissolution process. As reported in the literature [31,47], both phenomena can be described using a kinetic model, represented by the following equation:

$$\frac{dW}{dt} = -k_{eff} W^n \tag{1}$$

Thus, integrating:

$$W = [W_0^{1-n} - (1-n)k_{eff} t]^{\frac{1}{1-n}} \tag{2}$$

where k_{eff} is the global reaction rate coefficient, which accounts for all the mass transfer phenomena occurring during the process, W_0 is the weight of the sample before the depolymerization process, and n is the order of the model (assumed equal to 2). The parameter k_{eff} was varied to fit data and minimize the root mean square error (RMSE).

3. Numerical part

3.1. Model for cure kinetics and voids growths

In our study, we aimed to correlate manufacturing conditions with the quality of composite materials intended for recycling. We specifically focused on two critical properties: the degree of cure (α) and the representative void radius (R_V). By varying the manufacturing conditions, we sought to simulate the behavior of end-of-life composites, which can experience localized chemical and physical deterioration, such as porosity, due to exposure to their service environment and repair operations [1,48,49]. To estimate the degree of cure and void radius for the composites cured under the examined conditions, we utilized a

Table 3
Characteristics of voids in samples under various curing processing conditions. The voids are assumed to be spherical and occupy 3% of the sample's volume.

Processing conditions for samples manufacturing	R_V(μm)	Number of voids (10^3)	Total voids surface (mm^2)
7 h – 65 °C	31.8	150	1913
7 h – 50 °C	31.2	159	1950
72 h – 23 °C	30.0	179	2028

MATLAB code developed based on prior research [48]. This code incorporates models for cure kinetics and void size evolution. The void size generated by the code is interpreted as the mean void size within a randomly distributed spherical void system. To ensure that the volume fraction of voids reaches a typical content of 3 % for composites [50,51], we calculate the number of voids to be included in the representative volume element for subsequent analyses. The model simulates an ambient pressure curing process, beginning at room temperature (23 °C) and progressing to a specified target temperature, while accounting for the rate of temperature increase during the curing process. Other key parameters in the model include the activation energy E_a and the initial void radius R_0, both of them which were determined based on existing literature and known data. Specifically, E_a was set at 62.3 kJ/mol to align with the cure times provided in the datasheet at given temperature profiles. Meanwhile, R_0 was assumed to be 30 μm, as supported by previous works [48]. Fig. 2 illustrates the evolution of both the degree of cure and the void radius as a function of curing time, based on the model developed by Paul et al.[48], across the various curing schemes employed in this study. We observe that different degrees of cure are achieved with each processing condition. PC 1 yields an α value of approximately 0.96, while both PC 2 and PC 3 result in α values of around 0.90. This indicates that PC 1 are more effective in promoting cross-linking in the material, whereas PC 2 and PC 3 leave a larger portion of the material uncured. Regarding the void radius, the number of voids, and the extent of the void's surfaces, values are detailed in Table 3. It is found that the surface area of the voids increases from PC 1 to PC 2 and then to PC 3. Due to the combination of more under-cured regions and an increased void-solvent contact area, a progressively higher overall solvolysis rate can be expected when transitioning from PC 1 to PC 2, and subsequently to PC 3. A lower degree of cure leads to a less cross-linked polymer network, enhancing the mobility of solvent molecules within the material. Additionally, the larger void-solvent contact area improves solvent penetration and interaction with the polymer matrix. These factors work together to accelerate solvolysis by

Table 4
Parameters used in the computational model to simulate the solvolysis of epoxy samples.

Parameter	Description	Value	Unit
D_0	Reference diffusivity	3×10^{-6}	mm^2/s
β	Constant for diffusivity	0.95	
E	Constant related to the dependence of temperature	3×10^6	mJ/mol
E_a	Activation energy	1.3×10^4	mJ/mol
B	Constant for the rate of dissolution	5×10^3	mm^3/mol
c_0	Constant solvent concentration in the system	1.8×10^{-5}	mol/mm^3
A	Frequency factor	0.1	

facilitating the breakdown of polymer bonds more efficiently.

3.2. Numerical modeling strategy

A computational model based on a phenomenological approach, incorporating both diffusion and dissolution components [44], was employed to describe the solvolysis process. Diffusion is typically simulated by heat transfer analysis, leveraging the analogy between Fourier and Fick's laws [52]. The adopted model utilizes Fick's law to express the balance of solvent transport. The relevant partial differential equation is:

$$\frac{\partial c}{\partial t} = -D\nabla^2 c + H \tag{3}$$

where H represents the volumetric change rate of solvent concentration due to polymer dissolution, c is the solvent concentration (mol/m^3), and D is the diffusivity of solvent into the polymer (mm^2/s). The diffusivity D varies with both temperature and degree of dissolution [53,54], which can be expressed as:

$$D = D_0 e^{-(E/RT)} e^{\beta\alpha^2} \tag{4}$$

where D_0 is a reference diffusivity (mm^2/s), E is a constant indicating the dependence of temperature (kJ/mol), R is the universal gas constant (8.31 J/mol/K), T is the absolute temperature (K), β is a parameter related to the dissolution degree, and α is the extent of polymer dissolution ranging from 0 (polymer in solid state) to 1 (polymer completely dissolved). In this paper, when α exceeds 0.99, the dissolution is considered complete.

The rate of polymer dissolution is described by a modified solid-state reaction law [55]:

$$\frac{d\alpha}{dt} = Ag(c)e^{-(E_a/RT)}f(\alpha) \tag{5}$$

$$g(c) = 1 - e^{-Bc} \tag{6}$$

where, A represents the frequency factor and E_a is the activation energy. The function $g(c)$ defines the dependence on solvent concentration c, with B being a model parameter.

This model was implemented in the commercial finite element software package Abaqus 2022, using the subroutines USDFLD and HETVAL. Further details of the model can be found in the study by Chen et al. [44]. The model was calibrated using experiments on pure resin samples subjected to varying solvolysis temperatures. Subsequently, it was employed to simulate the dissolution of fiber-reinforced samples, considering the effects of voids and fiber volume fraction.

The parameters used in the numerical model were derived from solvolysis experiments conducted on resin samples cured under processing conditions of 65 °C for 7 h. A model with dimensions of 13 mm × 13 mm × 4 mm was created and meshed using 8-node trilinear displacement and temperature elements (C3D8T) in Abaqus 2022. A convergence analysis was performed, suggesting that convergence was achieved with a mesh of 50,700 elements. In the absence of diffusion tests and to streamline the process, model calibration was primarily focused on the parameters most significantly affecting the results. These key parameters include the diffusion coefficients (D_0 and E, as defined in Equation (4), the frequency factor A, and the activation energy E_a. The parameter values are provided in Table 4.

Assuming that the dissolution mechanism is expected to remain consistent across different sizes, in order to reduce the significant computational time required for complex geometries, the composite models were simplified to a thickness of 0.57 mm (one-seventh of the actual sample) with a length and width of 1 mm, as illustrated in Fig. 3b. The model consists of pure resin layers (beige) and composite layers, which include fibers (orange) and matrix (dark green) as represented in Fig. 3. Simulating the actual number of fibers is computationally intensive, requiring significant time and resources. To reduce this burden, the fiber structures are represented as an array of fiber bundles, with each bundle having a diameter approximately fourteen times larger

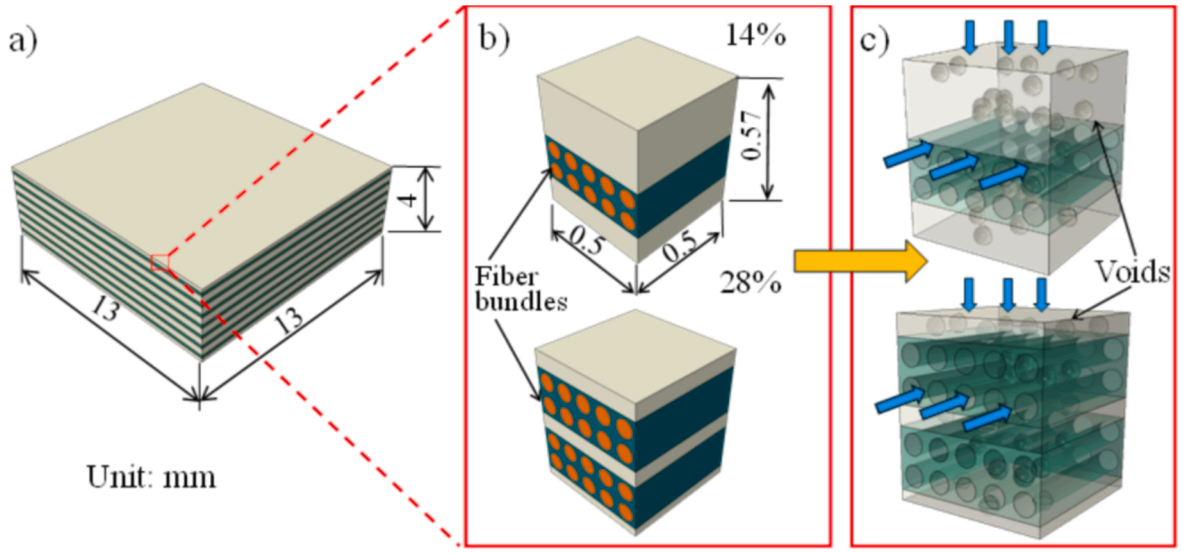

Fig. 3. Schematic of the composites dissolution models: real-size model consisting of composites and pure resin layers (a); scaled-down models used in simulations (b), with one-seventh of real-size model's height and fiber bundles; models with voids (c). Blue arrows indicate the initial diffusion starting from the top and front surfaces.

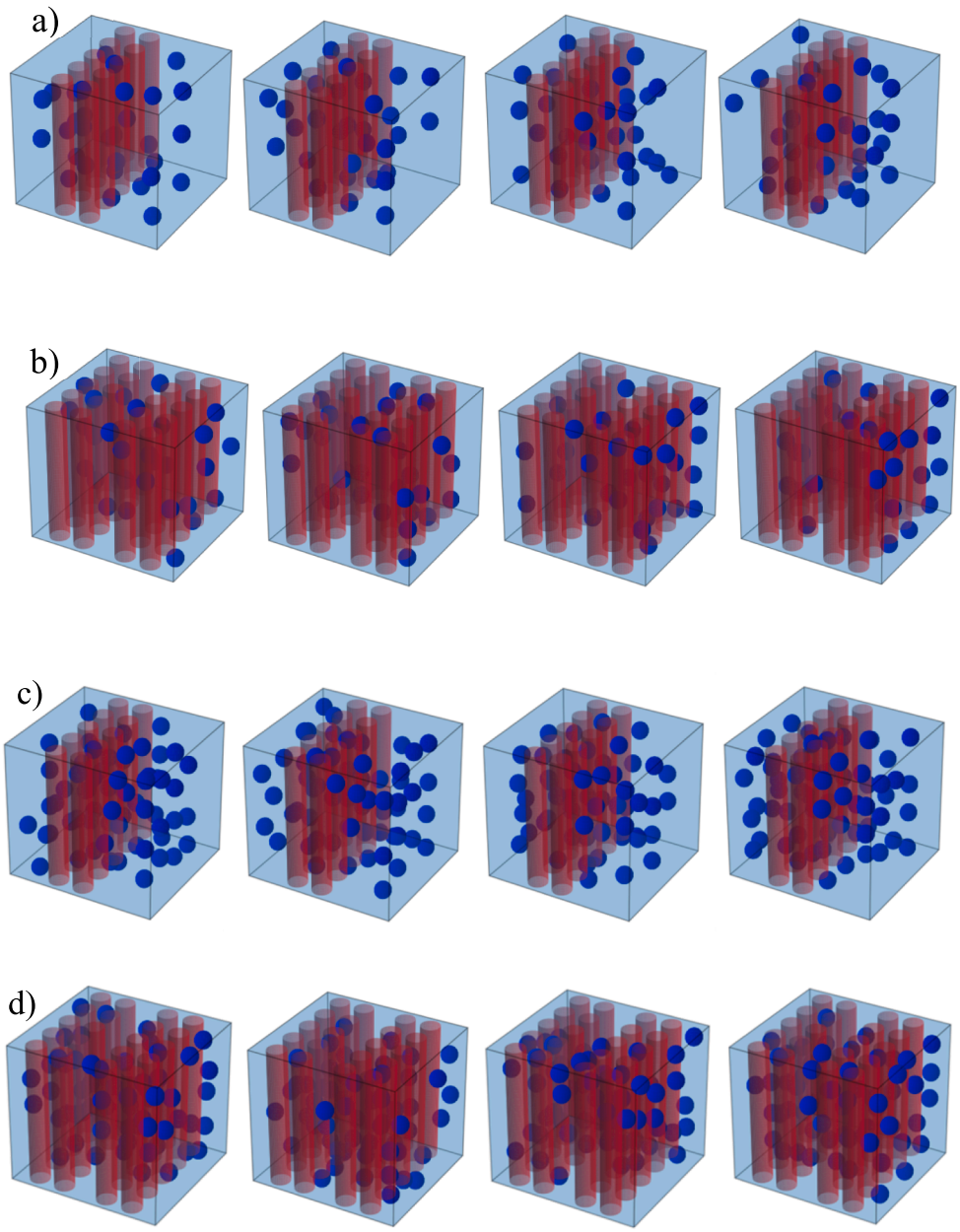

Fig. 4. Random distributions of voids: 3% voids content with fiber volume fractions of (a) 14% and (b) 28%, and 6% void content with fiber volume fractions of (c) 14% and (d) 28%.

than that of a single fiber (72 μm vs. 5 μm). The distance between the centers of two adjacent circles is 100 μm. Assuming no solvent transport or chemical reactions occur within the carbon fibers, the fiber bundles were treated as inert in the model. As for the case of neat resin, voids with a radius of 31.8 μm and a volume fraction of 3 % are expected in the sample cured with processing conditions PC 1 (7 h at 65 °C).

To investigate the impact of voids on composite dissolution and how this varies with different fiber volume fractions, two models with fiber contents of 14 % and 28 %, respectively, were analyzed. The volume fraction of voids in the analysis was 3 % and 6 %. Voids were randomly distributed by a random removal algorithm [56,69] (Fig. 3c). The algorithm initially generated voids within the composite model, ensuring that no voids were in direct contact with the fiber bundles. Subsequently, voids were randomly removed to achieve the target void content. To account for the inherent randomness and variability in the void distribution, the simulation was conducted four times for each fiber volume fraction, each run producing a distinct distribution of voids, as shown in Fig. 4. Since voids can be occupied by solvent during penetration, and the penetration time on a microscale is negligible, an initial solvent concentration is assumed to exist at the surface of the voids. Several studies have demonstrated that longitudinal diffusion is faster than transverse diffusion due to several factors: the more torturous path in the transverse direction [57], a fiber–matrix interphase with less dense crosslinking and local plasticization [58,59], and a weak or deboned interface between fibers and matrix [60]. In this study, we assume that the transverse and longitudinal diffusivities of the matrix in the composites layers have a linear relationship, as described by Kondo and Taki [61] and reported in Eq.7:

$$\begin{cases} D_T = 0.50 D_L, & V_f = 14\% \\ D_T = 0.45 D_L, & V_f = 28\% \end{cases} \tag{7}$$

where D_T and D_L are the transverse and longitudinal diffusivities, and V_f

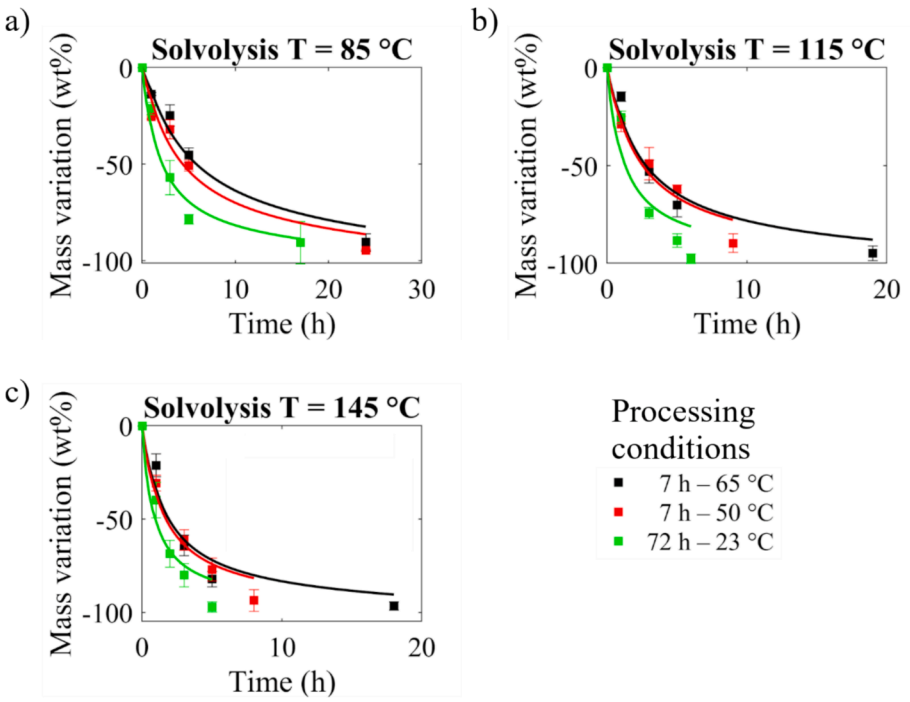

Fig. 5. Mass percentage variation of epoxy samples after solvolysis at temperature of 85 °C (a), 115 °C (b), and 145 °C (c) with concentration of 18 mol/L . Solid lines are the kinetic model fit.

is the volume fraction of the fibers. The diffusion is assumed to start from the top and front surfaces to study the anisotropic diffusion behaviors. The finite element discretization of the composite material models (Fig. 3b and 3c) was created using the preprocessor in Abaqus 2022. The models were meshed with 4-node linear displacement and temperature tetrahedron elements (C3D4T), using a comparable mesh size (the use of about 170,000 or more elements) determined by a convergence study. This element type was selected for its compatibility with the varying geometries to be meshed and its suitability for temperature conduction analysis.

4. Results and discussion

4.1. Effects of processing conditions on the yield rate of solvolysis

Epoxy samples depolymerization data are presented in Fig. 5, showing the weight percentage variation calculated after a certain treatment time relative to the pre-test weight of the same sample. This variation depends on the solvolysis temperature: 85 °C in Fig. 5a, 115 °C in Fig. 5b, and 145 °C in Fig. 5c, across the various manufacturing conditions of the treated samples. Experiments were conducted only at the highest concentration to reduce test times and isolate the effects of temperature. In all cases, composites cured with PC 1 exhibit the longest depolymerization times, while composites cured with PC 2 and especially PC 3 show faster solvolysis. This is likely due to the fact that the first set of processing conditions for curing corresponds to the datasheet values, whereas the other two involve lower temperatures. This results in a greater presence of under-cured regions and an increased void-solvent contact area (Section 3.1), which promote more rapid depolymerization.

The results indicate that increasing the temperature accelerates the solvolysis rate. Higher temperatures enhance both the diffusion of the solvent into the samples (Equation (4) and the rate of the depolymerization reaction [29]. The second-order kinetic model effectively captures the overall behavior of this phenomenon, with the root mean square error ranging from 5 % to 7 %, except for the of PC 3 at 115 °C, which exhibits an error of approximately 11 %. This higher error can be attributed to the combination of elevated temperature and lower composite quality, resulting in a faster and less predictable dissolution process. A significant discrepancy between the kinetic model and experimental data is observed during the early stages of solvolysis, at around 1 h, where the model predicts lower masses. This discrepancy may be attributed to the absorption of the solvolysis fluid by the samples, which occurs before there is sufficient time for depolymerization to take place. The times required to achieve 90–95 wt% depolymerization are summarized in Table 5. At a solvolysis temperature of 85 °C, both PC 1 and PC 2 samples required 24 h, while PC 3 samples took a shorter time of 17 h. Increasing the temperature reduced the treatment times. For PC 1 samples, the time decreased to 19 h at 115 °C and 18 h at 145 °C. A more significant reduction was observed for PC 2 samples, with the treatment time dropping from 24 h at 85 °C to 9 h at 115 °C and 8 h at 145 °C. For PC 3, the time decreased from 17 h at 85 °C to 6 h at 115 °C and 5 h at 145 °C.

Table 5
Final depolymerization times (in h) for samples cured under different processing conditions at various solvolysis temperatures. Percentage reductions are relative to the 85 °C case.

Processing conditions for samples manufacturing	Solvolysis temperature		
	85 °C	115 °C	145 °C
7 h – 65 °C	24	19 (−21 %)	18 (−25 %)
7 h – 50 °C	24	9 (−62 %)	8 (−67 %)
72 h – 23 °C	17	6 (−65 %)	5 (−71 %)

The next parameter analyzed was the molar concentration of the solvolysis fluid, which was reduced from 18 mol/L to 17 mol/L and 16 mol/L. Experiments, conduced for samples cured with PC 1 and treated at the solvolysis temperature of 115 °C indicate that a lower concentration result in a longer solvolysis time. Specifically, the time required to achieve maximum depolymerization increased from 19 h to 29 h (+53 %) at 17 mol/L, and to 48 h (+153 %) at 16 mol/L (Fig. 6). The second-order kinetic fitting shows a root mean square error ranging from 4.72 % to 6.21 %, indicating no significant difference in the model's

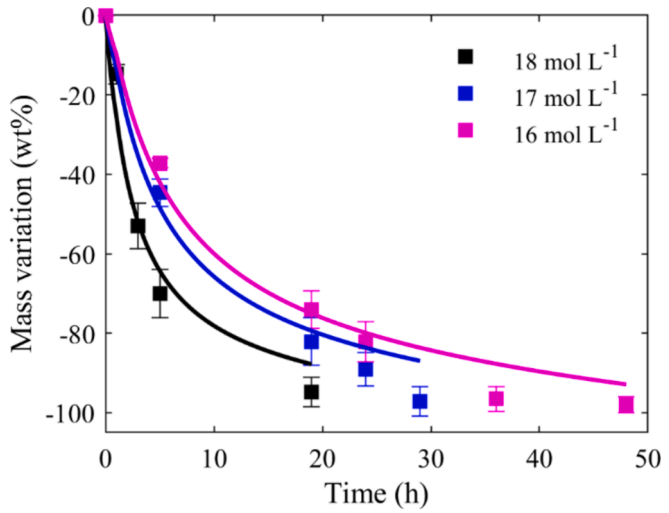

Fig. 6. Mass percentage variation of epoxy samples cured with PC 1 after solvolysis at concentration of 18 mol/L , 17 mol/L , and 16 mol/L , at a temperature of 115 °C with kinetic model (solid line).

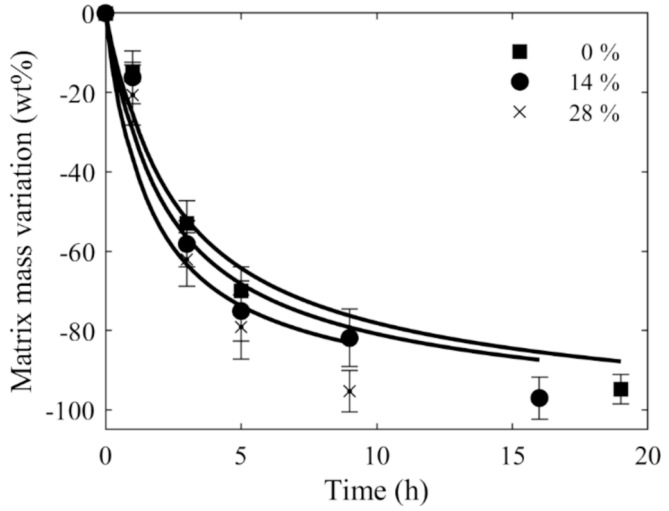

Fig. 7. Matrix mass percentage variation of composite samples cured with PC 1, with reinforcement volume fractions of 0 %, 14 %, and 28 %, after solvolysis at a concentration of 18 mol L^{-1} , with the kinetic model represented by the solid line.

accuracy across the analyzed cases.

Experiments were conducted for the PC 1–18 mol L^{-1}–T = 115 °C case to assess the influence of fiber volume fraction. The weight reduction of composite samples is compared to the results for neat epoxy samples (Fig. 7). For composites, the weight reduction is calculated relative to the polymeric portion of the samples, based on the known volume fraction of the reinforcements and the densities of both the matrix and the fibers.

Increasing the fiber content appears to accelerate solvolysis. The time required to achieve maximum depolymerization decreases from 19 h to 16 h (−16 %) for the 14 % fiber volume fraction (Vf) case, and to 9 h (−53 %) for the 28 % Vf case. This is because a higher fiber content results in a lower proportion of matrix material, thus reducing the time needed for complete depolymerization. Additionally, a greater fiber content enhances polymer dissolution by accelerating diffusion along the fibers, as discussed in Section 3.2. Furthermore, the incorporation of carbon fibers into the polymer matrix establishes distinct interfaces and interphases. These regions facilitate faster diffusion compared to the

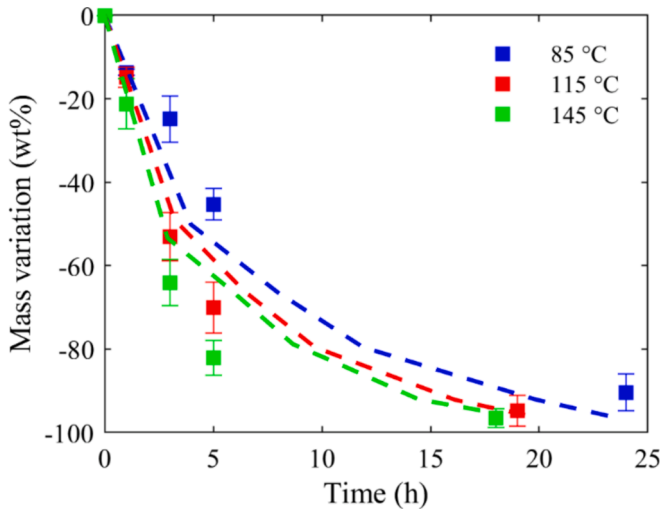

Fig. 8. Comparison of solvolysis process between experimental data and model (dashed lines) at solvolysis temperatures of 85 °C, 115 °C, and 145 °C for neat epoxy samples cured at 65 °C for 7 h (PC1).

bulk matrix, owing to the differences in material properties [44,62,63]. The root mean square error increases from 6.21 % for neat epoxy samples to 7.36 % and 9.25 % for the 14 % and 28 % Vf cases, respectively. This rise in error suggests that the model used to fit the experimental data is less suited for composites, due to the more variable diffusion and dissolution characteristics compared to neat epoxy samples.

4.2. Numerical modelling of epoxy solvolysis

Fig. 8 presents the results of fitting model to the dissolution process under varying solvolysis temperature conditions for neat resin samples manufactured with processing condition of 65 °C for 7 h. At solvolysis temperatures of 85 °C and 145 °C, the model's predictions diverge slightly from the experimental data after the 5-h mark, although they show convergence by the end of the observation period. The RMSE for the sample at 85 °C and 145 °C were 7.66 % and 9.77 %, respectively. This discrepancy likely arises from the complex relationship between diffusivity and temperature, which is not fully accounted for by the Arrhenius model. Such limitations of the Arrhenius model in describing the temperate dependence of diffusivity have been observed at high temperature levels [64] and in cases involving the diffusion of alkanes [65] and acids [66] in polystyrene. Another potential factor for the discrepancy is the nonlinearity of diffusivity. For instance, in studies of diffusion in phenolic resin-based composites-water systems [67], the diffusion rate through the composites was found to be highly sensitive to initial and final conditions. Hamel et al. proposed a reaction–diffusion model with nonlinear, concentration-dependent diffusion coefficients to more accurately describe the dissolution of thermosetting polymer [68]. To refine the understanding of diffusivity, additional diffusion experiments are necessary, particularly under varying temperature and concentration conditions. At a solvolysis temperature of 115 °C, the model demonstrates a strong agreement with the experimental data throughout the entire dissolution process, with a root mean square error of 6.16 %. Since the model accurately captures the dissolution behavior at this temperature, it was applied at 115 °C to investigate the effects of fiber reinforcement and voids on the dissolution process.

4.3. Numerical modelling of composites solvolysis

Fig. 9 shows the predicted solvolysis of composites with and without voids at different fiber volume fractions. Note that the curves representing the presence of voids are obtained by averaging the results from four simulations for each fiber volume fraction. Table 6 summarizes the

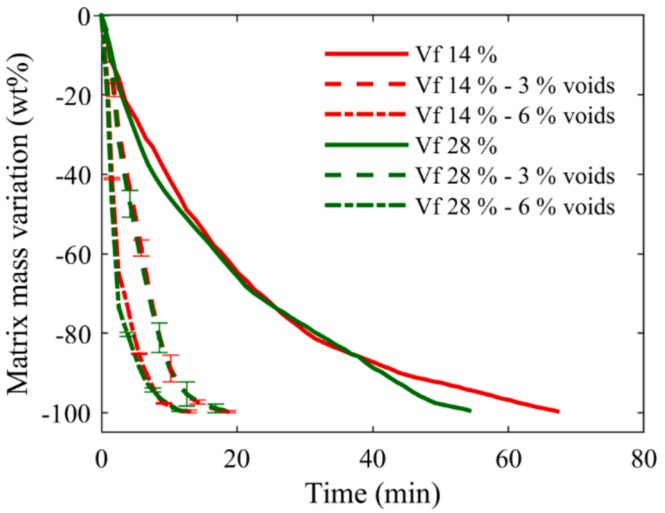

Fig. 9. Predicted solvolysis behavior of composites with varying void contents: 3% voids (dashed lines), 6% voids (dotted lines), and no voids (solid lines), across different fiber volume fractions.

Table 6
Simulated dissolution time for models with and without voids.

Vf	Void content	Dissolution time
14 %	–	67.55
14 %	3 %	19.75 ± 0.12
14 %	6 %	12.37 ± 0.31
28 %	–	54.55
28 %	3 %	19.08 ± 0.57
28 %	6 %	12.21 ± 0.17

average dissolution times for complete matrix dissolution, highlighting the effects of void content, void arrangement, and fiber volume fractions. The spatial arrangement of voids has a minimal impact on the dissolution process, as evidenced by the similar results observed across different fiber volume fractions (represented by dashed and dotted lines). Furthermore, the effects of void arrangement diminish significantly when the void content increases to 6 %. Overall, the data reveal that higher fiber volume fractions (28 %) result in faster dissolution rates compared to lower fiber volume fractions (14 %), regardless of the presence of voids. This observation aligns with the experimental results shown in Fig. 7. Furthermore, the increase in dissolution rate from 14 % to 28 % fiber volume fraction is more pronounced when voids are absent, exhibiting a 19.3 % improvement. In contrast, this rate of increase is reduced to 3.4 % and 1.3 % in the presence of 3 % and 6 % voids, respectively. The presence of voids accelerates the dissolution process for both fiber volume fractions, with the effect being more pronounced at the lower fiber volume fraction.

Fig. 10 presents the results for the composite materials with $V_f = 14$ % containing 3 % voids at various stages of the dissolution process. At 2 min, the composite exhibits early signs of faster dissolution along the fibers compared to the direction perpendicular to the fiber length. Solvent diffusion from the voids into the polymer causes the dissolution to spread around the voids, as shown in the yellow dashed rectangles in Fig. 10. By 4 min, the solvent has penetrated further from the voids, leading to more extensive dissolution. The simulation indicates that defects, such as voids in composite materials, significantly affect the chemical recycling process, with this effect being more pronounced at lower fiber volume fractions. Understanding the role of voids and their relationship with solvolysis can enhance the efficiency of recycling composite materials, contributing to more sustainable lifecycle management of composites.

5. Conclusions

This study investigated the effects of manufacturing-induced defects such as voids and solvolysis conditions on the chemical recycling of epoxy-based carbon fiber composites. Key factors include uncured regions and increased porosity, both of which promote faster depolymerization. A lower degree of cure results in fewer cross-links, making the material less resistant to solvents. Additionally, a higher number of voids increases the surface area available for interaction with the solvent, thereby accelerating the process. The presence of carbon fiber reinforcement at the studied percentages also enhances solvolysis due to the reduced amount of matrix material that needs to be depolymerized and the faster diffusion of the solvent along the fibers. Furthermore, the analysis of solvolysis parameters revealed that increasing the temperature enhances the overall speed of the process by improving the solvent's diffusivity into the polymer. Conversely, reducing the solvent concentration slows the process, as the fluid's depolymerizing power diminishes.

A computational model incorporating both diffusion and dissolution components was developed and calibrated with experiments on pure epoxy samples, showing favorable agreement with the experimental data. The model's application to scaled-down structures with fiber bundles and anisotropic diffusion coefficients confirmed that manufacturing-induced voids accelerate the solvolysis process, especially at lower fiber volume fractions. These findings underscore the importance of understanding the role of voids and the relationship between porosity and solvolysis in enhancing the recycling efficiency of composite materials.

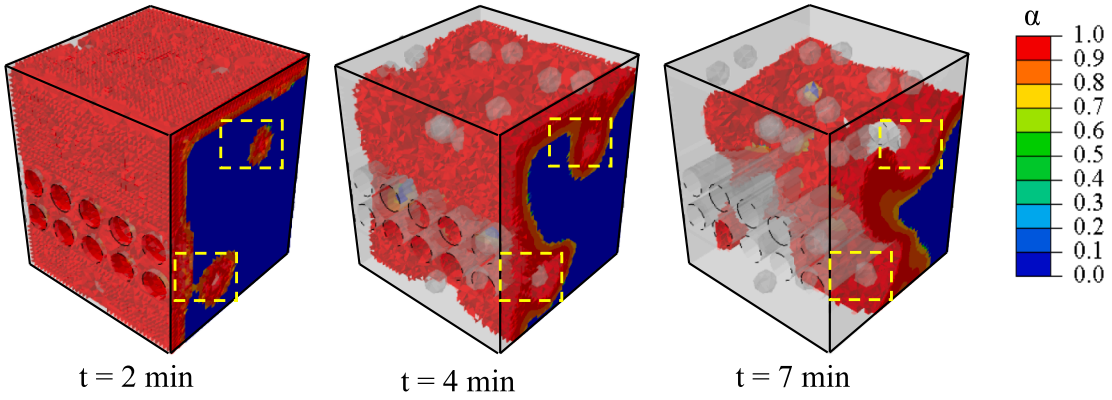

Fig. 10. Predicted appearance at various times for the dissolution process of the composites with the voids content of 3% and fiber volume fraction of 14%. The contour colors show the extent of polymer dissolution α (Equation (5)).

CRediT authorship contribution statement

Daniele Tortorici: Writing – original draft, Validation, Investigation, Formal analysis, Data curation, Conceptualization. **Yi Chen:** Writing – original draft, Validation, Investigation, Formal analysis, Data curation, Conceptualization. **Leon Mishnaevsky:** Writing – review & editing, Validation, Supervision, Resources, Methodology, Funding acquisition, Conceptualization. **Susanna Laurenzi:** Writing – review & editing, Validation, Supervision, Resources, Methodology, Funding acquisition, Conceptualization.

Declaration of competing interest

The authors declare that they have no known competing financial interests or personal relationships that could have appeared to influence the work reported in this paper.

Acknowledgement

The authors Y.C. and L.M. acknowledge the financial support of the Innovation Fund Denmark in the framework of project "WiseWind: New generation of sustainable wind turbine blades" (wisewind.dtu.dk/), No.2079-00004B.

L.M. is grateful to the European Commission for the support in the framework of Horizon project "Blades2Build: Recycle, repurpose and reuse end-of-life wind blades composites: A coupled pre- and co- processing demonstration plant", grant agreement 101096437 and to the Ministry of Foreign Affairs of Denmark via Danida grant 19-M02-DTU "Maintenance and repair strategy for wind energy development" (maintainergy.dk).

Data availability

Data will be made available on request.

References

[1] Smith WF, Hashemi J. Foundations of materials science and engineering. Mcgraw-Hill Publishing; 2006.
[2] Godara SS, Yadav A, Goswami B, Rana RS. Review on history and characterization of polymer composite materials. Mater Today Proc 2021;44:2674–7. https://doi.org/10.1016/j.matpr.2020.12.680.
[3] Vasiliev VV, Morozov EV. Advanced mechanics of composite materials and structural elements. Newnes; 2013.
[4] Laurenzi S, Casini A, Pocci D. Design and fabrication of a helicopter unitized structure using resin transfer moulding. Compos Part A Appl Sci Manuf 2014;67:221–32. https://doi.org/10.1016/j.compositesa.2014.09.007.
[5] Mishnaevsky L, Branner K, Petersen HN, Beauson J, McGugan M, Sørensen BF. Materials for wind turbine blades: an overview. Materials 2017. https://doi.org/10.3390/ma10111285.
[6] Sarfraz MS, Hong H, Kim SS. Recent developments in the manufacturing technologies of composite components and their cost-effectiveness in the automotive industry: a review study. Compos Struct 2021;266:113864. https://doi.org/10.1016/j.compstruct.2021.113864.
[7] Tortorici D, Sabatini M, Laurenzi S. Numerical simulations and experimental results of the deployment of thin-walled bistable composite booms. Compos Struct 2024;327:117669. https://doi.org/10.1016/j.compstruct.2023.117669.
[8] Phoenix S. Modeling the statistical lifetime of glass fiber/polymer matrix composites in tension. Compos Struct 2000;48:19–29. https://doi.org/10.1016/S0263-8223(99)00069-0.
[9] Spini F, Bettini P. End-of-Life wind turbine blades: review on recycling strategies. Compos B Eng 2024;275:111290. https://doi.org/10.1016/j.compositesb.2024.111290.
[10] H. Jiang, Trends in fleet and aircraft retirement, in, https://www.aviationsuppliers.org/ASA/files/ccLibraryFiles/Filename/000000001327/GS%20Tues%20-%20Jiang.pdf, 2015.
[11] Liu P, Barlow CY. Wind turbine blade waste in 2050. Waste Manag 2017;62:229–40. https://doi.org/10.1016/j.wasman.2017.02.007.
[12] Arulprasanna A, Omkumar M. A review on composites: Selection and its applications. Mater Today Proc 2024. https://doi.org/10.1016/j.matpr.2024.06.014.
[13] Tanks JD, Arao Y, Kubouchi M. Diffusion kinetics, swelling, and degradation of corrosion-resistant C-glass/epoxy woven composites in harsh environments. Compos Struct 2018;202:686–94. https://doi.org/10.1016/j.compstruct.2018.03.078.
[14] Zhang H-L, Liu J-Y, Zuo X-B, Tian J-L, Zou Y-X. A composite epoxy coating with a newly synthetic BN@SiO2 filler and its improvement on the durability of cement-based materials. Constr Build Mater 2023;404:133272. https://doi.org/10.1016/j.conbuildmat.2023.133272.
[15] Wong K, Rudd C, Pickering S, Liu X. Composites recycling solutions for the aviation industry. Sci China Technol Sci 2017;60:1291–300. https://doi.org/10.1007/s11431-016-9028-7.
[16] Arif ZU, Khalid MY, Ahmed W, Arshad H, Ullah S. Recycling of the glass/carbon fibre reinforced polymer composites: a step towards the circular economy. Polym -Plast Technol Mater 2022;61:761–88. https://doi.org/10.1080/25740881.2021.2015781.
[17] Rani M, Choudhary P, Krishnan V, Zafar S. A review on recycling and reuse methods for carbon fiber/glass fiber composites waste from wind turbine blades. Compos B Eng 2021;215:108768. https://doi.org/10.1016/j.compositesb.2021.108768.
[18] Sukanto H, Raharjo WW, Ariawan D, Triyono J. Carbon fibers recovery from CFRP recycling process and their usage: a review. IOP Conf Ser: Mater Sci Eng 2021;1034:012087. https://doi.org/10.1088/1757-899X/1034/1/012087.
[19] Ramawat N, Sharma N, Yamba P, Sanidhi MAT. Recycling of polymer-matrix composites used in the aerospace industry-a comprehensive review. Mater Today: Proc 2023. https://doi.org/10.1016/j.matpr.2023.05.386.
[20] Pickering SJ. Recycling technologies for thermoset composite materials—current status. Compos Part A Appl Sci Manuf 2006;37:1206–15. https://doi.org/10.1016/j.compositesa.2005.05.030.
[21] Oliveux G, Dandy LO, Leeke GA. Current status of recycling of fibre reinforced polymers: Review of technologies, reuse and resulting properties. Prog Mater Sci 2015;72:61–99. https://doi.org/10.1016/j.pmatsci.2015.01.004.
[22] Pietroluongo M, Padovano E, Frache A, Badini C. Mechanical recycling of an end-of-life automotive composite component. Sustain Mater Technol 2020;23. https://doi.org/10.1016/j.susmat.2019.e00143.
[23] Mamanpush SH, Li H, Tabatabaei AT, Englund K. Heterogeneous thermoset/thermoplastic recycled carbon fiber composite materials for second-generation composites. Waste Biomass Valoriz 2021;12:4653–62. https://doi.org/10.1007/s12649-021-01341-0.
[24] Giani N, Mazzocchetti L, Benelli T, Picchioni F, Giorgini L. Towards sustainability in 3D printing of thermoplastic composites: evaluation of recycled carbon fibers as reinforcing agent for FDM filament production and 3D printing. Compos Part A Appl Sci Manuf 2022;159:107002. https://doi.org/10.1016/j.compositesa.2022.107002.
[25] Palola S, Laurikainen P, García-Arrieta S, Goikuria Astorkia E, Sarlin E. Towards sustainable composite manufacturing with recycled carbon fiber reinforced thermoplastic composites. Polymers 2022. https://doi.org/10.3390/polym14061098.
[26] Xu M-X, Meng X-X, Ji H-W, Yang J, Di J-Y, Wu Y-C, et al. Evolution of pyrolysis char during the recovery of carbon fiber reinforced polymer composite and its effects on the recovered carbon fiber. J Environ Chem Eng 2024;12:112214. https://doi.org/10.1016/j.jece.2024.112214.
[27] Kawajiri K, Kobayashi M. Cradle-to-Gate life cycle assessment of recycling processes for carbon fibers: a case study of ex-ante life cycle assessment for commercially feasible pyrolysis and solvolysis approaches. J Clean Prod 2022;378:134581. https://doi.org/10.1016/j.jclepro.2022.134581.
[28] Rijo B, Dias APS, Carvalho JPS. Recovery of carbon fibers from aviation epoxy composites by acid solvolysis. Sustain Mater Technol 2023;35. https://doi.org/10.1016/j.susmat.2022.e00545.
[29] Tortorici D, Clemente R, Laurenzi S. Solvolysis process for recycling carbon fibers from epoxy-based composites. Macromol Symp 2024. https://doi.org/10.1002/masy.202400039.
[30] Shetty S, Pinkard BR, Novosselov IV. Recycling of carbon fiber reinforced polymers in a subcritical acetic acid solution. Heliyon 2022;8. https://doi.org/10.1016/j.heliyon.2022.e12242.
[31] Piñero-Hernanz R, Dodds C, Hyde J, García-Serna J, Poliakoff M, Lester E, et al. Chemical recycling of carbon fibre reinforced composites in nearcritical and supercritical water. Compos Part A Appl Sci Manuf 2008;39:454–61. https://doi.org/10.1016/j.compositesa.2008.01.001.
[32] Cheng H, Huang H, Zhang J, Jing D. Degradation of carbon fiber-reinforced polymer using supercritical fluids. Fibers Polym 2017;18:795–805. https://doi.org/10.1007/s12221-017-1151-4.
[33] Kooduvalli K, Unser J, Ozcan S, Vaidya UK. Embodied Energy in Pyrolysis and Solvolysis Approaches to Recycling for Carbon Fiber-Epoxy Reinforced Composite Waste Streams. Recycling 2022. https://doi.org/10.3390/recycling7010006.
[34] Wagner W, Pruß A, The IAPWS, formulation. for the thermodynamic properties of ordinary water substance for general and scientific use. Journal of physical chemical reference data 1995;31(2002):387–535. https://doi.org/10.1063/1.1461829.
[35] Khalil YF. Sustainability assessment of solvolysis using supercritical fluids for carbon fiber reinforced polymers waste management. Sustain Prod Consum 2019;17:74–84. https://doi.org/10.1016/j.spc.2018.09.009.
[36] Shuaib NA, Mativenga PT. Carbon Footprint Analysis of Fibre Reinforced Composite Recycling Processes. Procedia Manuf 2017;7:183–90. https://doi.org/10.1016/j.promfg.2016.12.046.
[37] Meng F, Olivetti EA, Zhao Y, Chang JC, Pickering SJ, McKechnie J. Comparing Life Cycle Energy and Global Warming Potential of Carbon Fiber Composite Recycling Technologies and Waste Management Options. ACS Sustain Chem Eng 2018;6:9854–65. https://doi.org/10.1021/acssuschemeng.8b01026.
[38] Oliveux G, Bailleul J-L, Gillet A, Mantaux O, Leeke GA. Recovery and reuse of discontinuous carbon fibres by solvolysis: Realignment and properties of

remanufactured materials. Compos Sci Technol 2017;139:99–108. https://doi.org/10.1016/j.compscitech.2016.11.001.
[39] Hao C, Zhao B, Shao L, Cao Y, Fei M, Liu W, et al. Mild chemical recycling of carbon fiber-reinforced epoxy composites in aqueous buffers and development of hydrothermally recyclable vitrimer composites from recyclates. Resour Conserv Recycl 2024;207:107668. https://doi.org/10.1016/j.resconrec.2024.107668.
[40] Lin X, Zheng L, Wang X, Xu P, Zeng C, Liao M, et al. Investigation of recycled carbon fiber-reinforced ultrafine-grain carbon-matrix composites. Sustain Mater Technol 2024;41. https://doi.org/10.1016/j.susmat.2024.e01033.
[41] Huang H, Liu W, Liu Z. An additive manufacturing-based approach for carbon fiber reinforced polymer recycling. CIRP Ann Manuf Technol 2020;69:33–6. https://doi.org/10.1016/j.cirp.2020.04.085.
[42] Tortorici D, Toto E, Santonicola MG, Laurenzi S. Effects of UV-C exposure on composite materials made of recycled carbon fibers. Acta Astronaut 2024;220:367–73. https://doi.org/10.1016/j.actaastro.2024.05.004.
[43] Luo C, Chung C, Yu K. A diffusion-reaction computational study to reveal the depolymerization mechanisms of epoxy composites for recycling. Mater Today Sustainability 2023;23:100452. https://doi.org/10.1016/j.mtsust.2023.100452.
[44] Chen Y, Mishnaevsky L. Modeling the Solvolysis of Composite Materials of Wind Turbine Blades. Adv Eng Mater 2024. https://doi.org/10.1002/adem.202302150.
[45] Fernlund G, Wells J, Fahrang L, Kay J, Poursartip A. Causes and remedies for porosity in composite manufacturing. IOP Conf Ser Mater Sci Eng 2016;139:012002. https://doi.org/10.1088/1757-899X/139/1/012002.
[46] Faisal MFM, Hassan A, Wui GK. Effects of sulphuric acid concentrations during solvolysis process on the mechanical properties of recycled carbon fiber. Sains Malays 2019:7. https://doi.org/10.17576/jsm-2020-4909-05.
[47] Mazich KA, Rossi G, Smith CA. Kinetics of solvent diffusion and swelling in a model elastomeric system. Macromol 1992;25:6929–33. https://doi.org/10.1021/ma00051a032.
[48] Paul D, Varshney A, Mahajan P, Mishnaevsky L. Post-repair residual stresses and microstructural defects in wind turbine blades: Computational modelling. Int J Adhes Adhes 2023;123:103356. https://doi.org/10.1016/j.ijadhadh.2023.103356.
[49] Mishnaevsky L, Frost-Jensen Johansen N, Fraisse A, Fæster S, Jensen T, Bendixen B. Technologies of Wind Turbine Blade Repair: Practical Comparison. Energies 2022. https://doi.org/10.3390/en15051767.
[50] Lambert J, Chambers AR, Sinclair I, Spearing SM. 3D damage characterisation and the role of voids in the fatigue of wind turbine blade materials. Compos Sci Technol 2012;72:337–43. https://doi.org/10.1016/j.compscitech.2011.11.023.
[51] Liu L, Zhang B-M, Wang D-F, Wu Z-J. Effects of cure cycles on void content and mechanical properties of composite laminates. Compos Struct 2006;73:303–9. https://doi.org/10.1016/j.compstruct.2005.02.001.
[52] Laurenzi S, Albrizio T, Marchetti M. Modeling of Moisture Diffusion in Carbon Braided Composites. International Journal of Aerospace Engineering 2008;2008:294681. https://doi.org/10.1155/2008/294681.
[53] Clague DS, Phillips RJ. Hindered diffusion of spherical macromolecules through dilute fibrous media. Phys Fluids 1996;8:1720–31. https://doi.org/10.1063/1.868884.
[54] Laidler KJ. The development of the Arrhenius equation. J Chem Educ 1984;61:494. https://doi.org/10.1021/ed061p494.
[55] Khawam A, Flanagan DR. Solid-state kinetic models: basics and mathematical fundamentals. J Phys Chem B 2006;110:17315–28. https://doi.org/10.1021/jp062746a.
[56] Park S-M, Lim JH, Seong MR, Sohn D. Efficient generator of random fiber distribution with diverse volume fractions by random fiber removal. Compos B Eng 2019;167:302–16. https://doi.org/10.1016/j.compositesb.2018.12.042.
[57] Barjasteh E, Nutt SR. Moisture absorption of unidirectional hybrid composites. Compos Part A Appl Sci Manuf 2012;43:158–64. https://doi.org/10.1016/j.compositesa.2011.10.003.
[58] Joliff Y, Rekik W, Belec L, Chailan JF. Study of the moisture/stress effects on glass fibre/epoxy composite and the impact of the interphase area. Compos Struct 2014;108:876–85. https://doi.org/10.1016/j.compstruct.2013.10.001.
[59] Mallarino S, Chailan JF, Vernet JL. Interphase investigation in glass fibre composites by micro-thermal analysis. Compos Part A Appl Sci Manuf 2005;36:1300–6. https://doi.org/10.1016/j.compositesa.2005.01.017.
[60] Gagani A, Krauklis A, Echtermeyer AT. Anisotropic fluid diffusion in carbon fiber reinforced composite rods: Experimental, analytical and numerical study. Mar Struct 2018;59:47–59. https://doi.org/10.1016/j.marstruc.2018.01.003.
[61] Kondo K, Taki T. Moisture Diffusivity of Unidirectional Composites. J Compos Mater 1982;16:82–93. https://doi.org/10.1177/002199838201600201.
[62] Herrmann A, Erich SJF, van der Ven LGJ, Huinink HP, van Driel WD, van Soestbergen M, et al. Interphase effect on the effective moisture diffusion in epoxy–SiO2 composites. Microelectron Reliab 2022;134:114550. https://doi.org/10.1016/j.microrel.2022.114550.
[63] VanLandingham MR, Dagastine RR, Eduljee RF, McCullough RL, Gillespie JW. Characterization of nanoscale property variations in polymer composite systems: 1. Experimental results. Compos Part A Appl Sci Manuf 1999;30:75–83. https://doi.org/10.1016/S1359-835X(98)00098-0.
[64] Elder RM, Saylor DM. Relations Between Dynamic Localization and Solute Diffusion in Polymers. J Phys Chem B 2021;125:9372–83. https://doi.org/10.1021/acs.jpcb.1c05010.
[65] Bernardo G. Diffusivity of alkanes in polystyrene. J Polym Res 2012;19:9836. https://doi.org/10.1007/s10965-012-9836-2.
[66] Bernardo G, Choudhury RP, Beckham HW. Diffusivity of small molecules in polymers: Carboxylic acids in polystyrene. Polymer 2012;53:976–83. https://doi.org/10.1016/j.polymer.2012.01.009.
[67] Alston S, Arnold C, Swan M, Stone C. A source-sink model for water diffusion in an activated carbon fiber/phenolic composite. Polym Compos 2021;42:3550–61. https://doi.org/10.1002/pc.26078.
[68] Hamel CM, Kuang X, Chen K, Qi HJ. Reaction-Diffusion Model for Thermosetting Polymer Dissolution through Exchange Reactions Assisted by Small-Molecule Solvents. Macromol 2019;52:3636–45. https://doi.org/10.1021/acs.macromol.9b00540.
[69] Kim Do-Won, Hyuk Lim Jae. Jaesang Yu. Efficient prediction of the electrical conductivity and percolation threshold of nanocomposites containing spherical particles with three-dimensional random representative volume elements by random filler removal. Composite Part B 2019;168:387–97. https://doi.org/10.1016/j.compositesb.2019.03.038.